Article:
Yang, K, Basheer, PAM, Bai, Y, Magee, B and Long, AE (2015) Assessment of the effectiveness of the guard ring in obtaining a uni-directional flow in an in situ water permeability test. Materials and Structures, 48 (1). pp. 167-183. ISSN 1359-5997

http://dx.doi.org/10.1617/s11527-013-0175-5

Assessment of the effectiveness of the guard ring in obtaining a uni-directional flow in an *in situ* water permeability test

Yang, K.[a], Basheer, P.A.M.[a], Bai, Y[b]., Magee, B[c]. and Long, A.E.[a]

[a] School of Planning, Architecture and Civil Engineering, Queen's University Belfast, Northern Ireland, UK

[b] Formerly at Queen's University Belfast, currently at Civil, Environmental and Geomatic Engineering, University College London, England, UK

[b] Formerly at Queen's University Belfast, currently at University of Ulster, Northern Ireland, UK

Corresponding Author:

Professor P.A. Muhammed Basheer

+44 28 9097 4026

m.basheer@qub.ac.uk

Abstract: The non-destructive evaluation of the water permeability of concrete structures is a long standing challenge, principally due to the difficulty of achieving a uni-direction flow for computing the water permeability coefficient. The use of a guard ring was originally proposed for the in-situ sorptivity test, but little information can be found for the water permeability test. In this study, the effect of a guard ring was carefully examined through the flow simulation, which was verified by carrying out experiments. It was observed that the guard ring can confine the flow near the surface, but cannot achieve a uni-directional flow across the whole depth of flow. To achieve a better performance, it is essential to consider the effects of the size of the inner seal and the guard ring and the significant interaction between these two. The analysis of the experimental data has indicated that the guard ring influences the flow for porous concretes, but there is no significant effect for dense concretes. Further investigation, validated using the flow-net theory, has shown a strong correlation between the water permeability coefficients obtained with the guard ring ($K_{w\text{-}GR}$) and without it ($K_{w\text{-}NO\ GR}$), suggesting that one dimensional flow is not essential for interpreting data for site tests. Another practical issue was that more than 30% of the tests with guard ring failed due to the

difficulty of achieving a good seal between the inner and the outer chambers. Based on the work reported in this paper, a new water permeability test is proposed.

Keywords: on-site water permeability test, guard ring, steady rate of flow, flow simulation

1. Introduction

The quality of concrete in structures should be assessed in situ because test specimens manufactured in the laboratory cannot accurately represent what happens in practice (Mehta and Monteiro 2006). Due to the link with the microstructure of concrete, permeation properties are considered as one key indicator of the durability of concrete (Neville 1996; Aïtcin 1998). As a result, permeation properties have become very popular in the recent past. Either 'dry' or 'saturated' samples are needed for measuring the transport properties. Dry conditions are preferred for the air permeability test, whereas saturated conditions are required for the water permeability test. Air permeability tests have become very popular, but the test specimens should be conditioned to remove the influence of moisture on test results (Parrott and Hong 1991; Basheer and Nolan 2001). It has been suggested that for normal concrete (NC) the internal relative humidity of the near surface concrete in the top 10mm depth should be less than 80% to yield reliable air permeability coefficients (Basheer and Nolan 2001). For high performance concretes (HPCs), the concrete specimens need to be dried in an oven at 40^{o}C at least for 3 weeks or an equivalent condition (Yang et al 2012). Such a moisture condition is not easy to achieve in situ, especially in most parts of northern Europe where annual rainfall averages from 80 to 110 mm (Perry and Hollis 2003). Therefore, it is logical that HPCs in structures should be tested when it is in a saturated condition rather than in a dry state. This means that in situ water permeability tests are preferable to air permeability tests for assessing the quality of HPC in structures.

Water permeability tests have been used to assess the permeability of concrete for more than 100 years (Hyde and Smith 1889). Many laboratory techniques have been developed and are accepted as international standards (BS-EN12390 2000; El-Dieb and Hooton 1995; Basheer 1991), but their field application is not so successful (Basheer 2001; TR-31 2008). One general concern is that a uni-directional flow that is needed for eliminating surface effects is

not easy to achieve on site and the water flow behaviour in the structure is much more complicated than that in the laboratory (Long et al. 2001; Torrent 1992).

To obtain a uni-directional flow, the application of a guard ring was proposed by Hall (1989) for the in-situ sorptivity (water absorption) test. Some researchers (Price and Bamforth 1993; Stanish et al. 2000) have incorporated this in the design of their instruments and the results were encouraging. Currently, only Torrent air permeability test (1992) uses a guard ring. However, the sorptivity and the air permeability tests would not provide reliable results when the concrete is wet and very little information can be found about water permeability tests with a guard ring. In addition, the exact influence of the contributory factors (size of a guard ring, the width of the inner seal and the outer seal, etc.) on the uni-directional flow is largely unknown, perhaps due to the difficulties in measuring the path of the water flow.

The simulation using flow-nets is one approach to solve the above issue (Bamforth 1987; Adams 1986). A similar approach was used to assess the influence of the guard ring in an in situ water permeability test that is reported in this paper. The design of the new water permeability test instrument was based on the CLAM water permeability test developed at Queen's University Belfast (Long 1985; Adams 1986). Before manufacturing the instrument, the performance of different test set-ups was investigated through a model study (reported in section 2). On the basis of this, a suitable arrangement was selected to give the desired performance and the instrument was then designed and manufactured. Once the test instrument was ready, experiments were carried out to verify its operation (reported in section 3). Analytically, the new water permeability test was studied using the flow-net theory under saturated steady rate of flow conditions. Two parameters were examined first, viz. the calibration factor and the steady flow rate. Then, the water permeability coefficient was evaluated according to the flow-net theory. The influence of the guard ring was assessed through comparing the permeability coefficients determined from the tests with and without using the guard ring. The merits and drawbacks of using the guard ring were then estimated. A new in-situ test for water permeability measurement was subsequently suggested for assessing the quality of concretes.

2. Development of the new *in situ* water permeability test

The first stage in the development of the new test was the identification of key factors affecting its performance with the guard ring. This was carried out analytically, by considering different design options and using the flow-net theory. The output from this was the basis of determining the effect of the different design options on the performance of the new water permeability test.

2.1 Details of the investigation to identify key factors affecting the performance of the new test with the guard ring

It is generally believed that a uni-directional flow is achieved if a guard ring is used (Nolan et al. 1997). Therefore, it was necessary to validate this hypothesis before developing the new water permeability test and, hence, the objective of this part of the research was to examine factors influencing the performance of the guard ring. The data thus obtained was used to decide the level of relevant parameters to obtain an effective and practical test set-up.

The factors which may affect the performance of an instrument with a guard ring depend on the configuration of the test head. Figure 1 shows details of a testing head with a guard ring. The relative dimensions of the testing area, the inner seal, the guard ring and the outer seal need to be specified before manufacturing the testing head.

The water flow can be described with an axis-symmetrical model when the water is applied over a circular area. Note that in this study the main emphasis was placed on investigating the effects of the size of the inner seal, the guard ring and the outer seal and hence, the other parameters were kept constant and were used as the input parameters (reported in Table 1). It consists of constant homogeneous permeability, full saturation of the pores and achievement of a steady flow rate. Three types of boundary conditions were defined in the model. The testing area and the guard ring had a constant pressure of 7 bar or 0.7 MPa (boundary condition 1). Both the inner seal and the outer seal were defined to have zero outflow of water (boundary condition 2). The potential seepage surface was the area beyond the outer seal of the test head (boundary condition 3). Figure 2(a) gives basic information for the model and Fig. 2(b) shows a typical output. The ‘10-30-20’ in this figure refers to the size of the

inner seal (10 mm), the size of the guard ring (30 mm) and the size of the outer seal (20 mm). The flow of water is described by the flow lines and the equi-potential lines. Therefore, an analysis of the flow-nets was used to study the behaviour of different setups, the results of which are presented in the next section. To study the influence of the three variables (the size of the inner seal, guard ring and the outer seal) on the uni-direction flow, the depth of uni-directional water flow was determined from the flow-nets.

2.2 Results of the model study on the performance characteristics of different setups

Figure 3 illustrates the procedure used to determine the uni-directional flow of water. The flow-net was constructed and the flow path (flow line) was drawn from the inner corner of the inner seal. Then, a reference line was drawn at the same position (the vertical line parallel to the flow line in Fig. 3). As can be seen, the comparison between this line and the flow line enables the identification of the depth of the uni-directional water flow.

The nine different setups for the variables in Table 2 resulted in a total of 9 models. Figure 2b and 5 shows the outputs of the nine models. Obviously, the flow patterns vary with different sizes of three factors (the inner seal, guard ring and the outer seal sizes), emphasising the importance of understanding their effects.

Figure 6 shows the uni-directional depth for each case. It can be seen that, when the inner seal was 15 mm, the depth of uni-directional water flow was less than 10mm for both 10 mm and 50 mm guard ring size and increasing the outer seal size from 10 mm to 30 mm did not have any noticeable effect. Although the increase in size of the guard ring from 10 mm to 50 mm did show an increase in depth of water flow, it was only marginal. The depth increased slightly (just above 10 mm) when the size of the inner seal was changed from 15 mm to 5 mm and the guard ring size was 10 mm. However, the depth of uni-directional water flow was around 25 mm when the size of the guard ring was increased to 50 mm. In both cases of the guard ring size, the increase in outer seal from 10 mm to 30 mm had only a marginal effect on the depth. This means that a deeper uni-directional water flow can be achieved with a guard ring test head by reducing the size of the inner seal and simultaneously increasing the size of the guard ring.

The main effect and the interaction effects of the factors were obtained by following the procedure for the central point factorial experiment design (Montgomery 1996). These are presented in Figs. 7 and 8. The main effects in Fig. 7 confirm the observation from Fig. 6 that an increase in the size of both the inner seal and the guard ring resulted in an increase in the response whereas the size of the outer seal had only a marginal response. At the heart of the concept of a guard ring, the central part of the flow below the guard ring should be as close as possible to the uni-directional flow. Therefore, it is not surprising to see that an increase in the size of the guard ring has a positive contribution to the response. The influence of the outer seal is marginal, because only small variations took place when the out seal size changed.

The two-way interactions between the three factors are shown in Fig. 8, indicating that the interaction between the inner seal and the guard ring is strong (divergent nature of the two lines). As other curves are nearly parallel in the other two plots, it is concluded that there are no interactions between the factors in these two plots. That is, the size of the guard ring should be decided based on the size of the inner seal and both these are independent of the size of the outer seal. The above results indicate that the guard ring confines the flow from the inner test area effectively and ensures a deeper uni-directional water flow when the thickness of the inner seal is small, and this beneficial effect decreases rapidly with an increase in the size of the inner seal.

Table 3 gives the statistical test results of the main effects and the interactions. The corresponding coefficients (Coef) of the model to predict the uni-direction depth were reported along with the estimated error (SE Coef). The results further confirm the above interpretation about the three factors and allow an equation to deduce the uni-directional flow depth (D):

$$Log(D) = 1.208 - 0.183 \times IS + 0.12 \times GR + 0.015 \times OS - 0.065 \times IS \times GR \quad (1)$$

The computer simulation also shows that an entirely uni-directional flow through the whole specimen is impossible despite the use of a guard ring, although this can be obtained near the surface. The water penetration depth of high performance concrete is in the range of 10 to 20 mm (Basheer 2001; TR-31 2008) and based on Equation 1, the size of the inner seal IS, guard

ring GR and the outer seal OS is suggested to be 5 mm, 30 mm and 20 mm respectively, giving a 20 mm deep uni-directional water flow.

3. Experimental validation of the new water permeability test

The water flow through a saturated porous material is described by the flow-net and its graphical properties can be used to obtain the analytical solution for the surface mounted water permeability test as that for the CLAM (Adams 1986; Arbaoui 1988). This can be expressed by:

$$K = q\frac{1}{2\pi h_t} \times \frac{n_d}{n_f} \times \frac{l}{rb} = q \times C \qquad (2)$$

where K is the coefficient of water permeability (m/s); q denotes the total flow (m^3/s); h_t denotes the head applied (m); n_f denotes the number of paths (flow channels); n_d denotes the number of equipotential drops; r is the distance normal to symmetry axis (m); b is the width of flow path (m); l is the distance between equipotentials (m); $\frac{1}{2\pi h_t} \times \frac{n_d}{n_f} \times \frac{l}{rb}$ is considered as a calibration factor (C).

The main benefit of using this theoretical approach is that any flow system can be simulated because the determination of the coefficient of water permeability is independent on achieving a uni-directional flow. Therefore, the flow through concrete for the new instrument can also be based on this principle.

3.1 Variables investigated

The primary aim of this part of the research was to ascertain if a uni-directional flow can be established using the guard ring and the axi-symmetric flow-net theory can be applied for both with and without the guard ring. To achieve this objective, several variables were examined, which are given in Table 4. As can be seen from this table, the experiment had 12 combinations of test conditions, which resulted from four concrete grades and three different curing regimes to provide a wide permeability range. Tests were conducted with and without

the guard ring for each concrete. The concrete mix proportions and the general properties (slump, air content and compressive strength) are reported in Table 5.

3.2 Manufacture of specimens

Nine 230×230×100 mm slabs were manufactured for each mix, which were divided into three groups for different curing regimes. The mixing procedure used in this research was based on BS-1881: part 125 (1986). Concrete was compacted using a table vibrator, where the mould was filled with concrete in two layers. The compaction was considered to have been completed when no air bubbles rose to the surface of concrete. The specimens were covered with wet hessian immediately after compaction and were removed from the mould after 24 hours. Then, they were cured as follows until the age of 90 days:

1) Designation AC: air-stored (20 ± 2 ^{o}C, 50 ± 10% RH) immediately after demoulding.
2) Designation WC: three-day water cured after demoulding and then moved to the controlled environment (20 ± 2 ^{o}C, 50±10% RH).
3) Designation SC: immersed in water (20 ± 1 ^{o}C) until test at the age of 90 days.

3.3 Preconditioning of the specimens

The flow-net theory is based on the acceptance of the validity of Darcy's law, for which saturated conditions and steady state of flow are required. Therefore, the specimens were saturated before carrying out the surface mounted new water permeability test. Note that the vacuum saturation was not used because the specimens were relatively large in size (230×230×100 mm). As it was established that incremental immersion can give results similar to that of vacuum saturation (Basheer and Nolan 2001), the slabs of AC and WC were saturated by incremental immersion when they were 90 days old. For this, the samples were placed with the test surface facing the bottom on supports in a plastic container, which was filled with water to 5 mm above the test surface for 2 days. Then, the water level was increased to half of the specimen thickness where they remained until the 5th day. The last stage was to raise the water level to the top of the specimen for 4 days. The samples continuously water cured (SC) were considered to be saturated, as they never left water after demoulding. The water permeability measurements were carried out on the bottom flat surface.

3.4 Design of the new *in situ* surface mounted water permeability test method

3.4.1 Description of the instrument

Figure 9 shows the schematic diagram of both set-ups; one with the guard ring and the other without. Both instruments have three main parts, which are a test head, a measuring body and a priming system. Most connections are the same for both arrangements. In comparison with the arrangements in Fig. 9(b) with the guard ring, the test without the guard ring used a different test head and the hydraulic cylinder for the guard ring was isolated by a ball valve, as shown in Fig. 9(a).

The test heads, the measuring unit and the priming system are shown in Fig. 10. Figure 10(a) details the test head with the guard ring that has two bleed valves (valve-2 and valve-3). The test head without the guard ring is shown in Fig. 10(b) and has only one bleed valve located at the centre of the head. The water tightness of the test head was checked before being clamped on the surface, which is shown in Fig. 10(c).

Figure 10(d) shows the measuring unit, which consists of three parts, a power supply, a display box and a testing unit. The testing unit is connected to the test head and the control box. It consists of two hydraulic cylinders, two pressure transducers and a voltage tracker. Two hydraulic cylinders are used to supply water to the test chamber and the guard ring respectively. The display box has a digital panel that shows the volume of water flowing into the concrete through the test area and the pressure levels at the test area and the guard ring (where this is present).

The water pressure is increased using the priming system, shown in Fig. 10(e). It comprises an air compressor, an air reservoir with a pressure gauge and a pressure regulator.

3.4.2 Procedure to carry out the new in-situ surface mounted water permeability test

Although similar procedures were used in both with and without the guard ring, for clarity each one is described below (the procedure for the test with the guard ring is given first).

1) The two cylinders of the test body were filled with water. Then, the test head was clamped on a specimen and water was admitted through the priming valve (valve 4) connected to the test region by using a syringe. The bleed valve (valve 2) was closed when water free from air bubbles appeared. This procedure was repeated for filling the chamber of the guard ring as well.
2) The test head was connected to the measuring unit and the priming system as shown in Fig. 9(a). The valves (valve-4 and valve-5 in Fig. 9(a)) of the priming system were closed initially, but valve-1 was kept opened. The air compressor was switched on and the air was pressurised in the air reservoir. The pump was turned off when the pressure gauge reading was slightly above 7 bar (0.7 MPa).
3) Valves 4 and 5 in the priming system were opened. The testing system was pressurised in both cylinders. After this, the two hydraulic cylinders were isolated by closing valve-1, indicated in Fig. 9(a).
4) The initial volume reading was recorded (t=0 min). At this test pressure water penetrated into the concrete, which resulted in a decrease of the pressure inside the two chambers. The pressure was maintained at 7 bar (0.7 MPa) by manually advancing the pistons through both chambers, which allowed the volume of water entering in to the concrete to be recorded at every minute.
5) The test was stopped after 120 minutes.

The operation of a test without the guard ring was easier, as there was no need to maintain the pressure in both chambers at the test pressure. Most steps of the procedure were the same (test pressure: 7 bar (0.7 MPa), duration: 120 min), with the following two differences:

1) A different test head that did not have the guard ring was used.
2) Only one cylinder that supplied water to the test region was used, whilst the other cylinder was closed by means of valve-3 in Fig. 9(b) before priming the system.

4. Results and discussion

4.1 Analytical evaluation of calibration factors

The calibration factor was estimated using the flow-net theory that was applied to determine the permeability coefficients. As shown in Fig. 11, the flow-net was affected by the use of a

guard ring. Based on Fig. 11, the calibration factors with and without the guard ring were calculated. The value for the test without the guard ring was 1.13×10^{-4} m^{-2}, which is in reasonable agreement with previous studies at Queen's University Belfast (Adams 1986; Arbaoui 1988). The calibration factor for the test with the guard ring was 4.25×10^{-4} m^{-2}. This means that the flow rate without the guard ring was 3.75 times higher than that with the guard ring due to the confinement of flow in the latter case. Bamforth (1987) gave a similar conclusion and suggested that the flow rate without any confinement is 4 times higher. The small difference is due to the fact that in Bamforth's case, the spread of flow was confined entirely by sealing the side surface, which is not the case for the surface applied water permeability test with the guard ring.

4.2 Method of determining the steady flow rate

Traditionally, a steady state flow rate is assumed in Darcy's law, which should satisfy the following two main requirements. The first one is that under the steady flow rate condition, a linear relationship exists between the volume of water penetrating into the concrete and the elapsed time. Secondly, no significant variation in the flow rates should exist during a specific period of time. Once these two conditions are satisfied, it can be assumed that a test has reached the steady-state. To assess if the steady flow rate was achieved, the following approach was used in this investigation:

1) Plot the volume against the elapsed time to get the initial information about the flow behaviours.
2) Determine the flow rates through regression analysis at interval of 15 minutes, which are displayed graphically. The relative change of flow rates is also given in another figure to compare the variation of flow rates.
3) Perform analysis of variance (ANOVA) to check if the flow has stabilised.
4) Draw conclusions.

Note that only one set of results (C20-SC-NO GR) was analysed and presented in this paper due to the similarity of the response for the other samples. The specimens (C20) were water cured for 90 days after demoulding and then the water permeability tests with and without the guard ring were carried out. In this section, the tests without the guard ring are presented and the results are analysed.

Figure 12(a) shows the volume of water against time and Fig. 12(b) shows the flow rate against time. From Fig. 12(a) it can be seen that the volume of water entering into the concrete has a non-linear relationship with time, which is in agreement with the results reported by El-Dieb and Hooton(1995) and Basheer (2001). As the specimens were water cured for 90 days and the test duration was 2 hours, it is highly unlikely that chemical reaction of unhydrated cement particles during the test played any significant role in this decrease of the flow rate (Basheer 2001; Hearn 1998). Numerous reasons could be assigned for this decrease in the flow rate in a high pressure water permeability test (TR-31, 2008), which includes silting of pores during the test and possible reduction of the gradient of pressure in concrete due to pressurisation of the pore water. From Fig. 12(b), the flow rate was found to decrease during the whole period of the test. However, significant reductions could be found during the initial period (< 60 min.). After 60 min, the rates were relatively close to each other and were less than 0.25 µl/min. It can be considered that the flow rates became almost constant after this time and the flow could be treated as steady-state.

The ANOVA was carried out so as to obtain statistical conformation to justify whether or not a significant difference existed between the flow rates during any 15 minutes interval after 60 minutes. In total, four flow rates were compared, which ranged from 60 min to 75 min, 75 min to 90 min, 90 min to 105 min, and 105 min to 120 min. Table 6 summarises the results of the ANOVA. It can be seen that the test statistic gave a value of 0.65 (corresponding to $F_{3,8}$ in Table 6) and the corresponding p-value was 0.604, much higher than 0.05. Therefore, this difference is not statistically significant at 5% level.

As the responses of other tests were very similar to this set of data, the steady flow rates under this condition were evaluated by regression analysis using the data after 60 minutes. Most of the flow rates reported in this work were obtained by this method except for C20 AC and C20 WC concretes, because the steady flow rate reached at an early test period for these two cases. Details are given in the next section.

4.3 Investigation of the influence of the guard ring

Figure 13 shows results of the water permeability tests with and without the guard ring. There were four types of concrete mixes and three curing regimes, with the primary focus on

investigating the influence of the guard ring on establishing a uni-directional flow. Note that different scales were used in the figure to show the effect of the guard ring.

Based on Fig. 13, the differences of volume of water flowing into the concrete are more than three orders of magnitude. This is reasonable as the water permeability coefficient often lies within several orders for different concretes (Neville 1996; Mehta and Monteiro 2006). Furthermore, most plots are curvilinear between volume and time, which is very similar to the results in Fig. 12. It means that a constant flow rate is almost impossible at the start of measurements, but after 60 minutes the volume is roughly proportional to the time. Consequently, the steady flow rates can be evaluated based on the method described in the previous section.

Note that two special cases were also found, which are C20 AC and C20 WC concretes. In these two cases, a linear relationship between the volume and the time was obtained from the start. In other words, constant flow rates were obtained before 60 minutes. El-Dieb and Hooton (1995) have reported that the duration to achieve the steady flow rate depends on the type of the concretes. As the pore structure of concrete is extremely complex (Cristensen et al. 1996; Mehta and Monteiro 2006), it is not possible for every pore to achieve the steady-state simultaneously. In general, the duration of steady flow rate depends on the size of pores and the flow in coarse pores stabilises faster than that in fine pores (Basheer 1991; Adams 1986). It is widely accepted that concrete with a high w/c ratio needs longer duration of moisture curing to obtain disconnected capillaries and curing for 3 days is not sufficient for concrete with w/c ratio higher than 0.6 (Neville 1996). Therefore, it can be deduced that the capillaries in C20 AC and C20 WC were coarse and interconnected. As a consequence, the flow through these two concretes was much higher than the rest and the steady flow rates (nearly constant flow rates) were reached within 5 minutes.

Two models were built to clarify the influence of the guard ring. In one model, the pressure was applied only in the test area, whereas in the other model the pressure was only applied in the guard ring. Figure 14 presents the flow-net for the two models. The flow patterns closer to the inner seal were enlarged so as to have a better view. It can be observed that the flow in the test area was restricted as the penetration depth of water front was approximately 2 mm under this test arrangement. Below 2 mm, the flow did not contact each other and, therefore, the guard ring had no effect on the flow from the test chamber.

It has been well established that air curing has an effect on permeability especially closer to the surface, because the moisture loss at the surface zone is faster (Dhir et al. 1989; Mehta and Monteiro 2006; Basheer 2001). In Fig. 13, for both C40 AC and C60 AC concretes the flow begins to diverge between tests with and without the guard ring after around 25 minutes, which is believed to be mainly caused by the coarse pores and higher permeability of the top surface produced by air curing. It takes 40 minutes for C40 WC to show the flow restriction caused by the guard ring. This is possibly due to the fact that a prolonged curing of concrete in water results in a better hydration, which in turn leads to less connected pores and low permeability (Hearn 1998). Both C20 AC and C20 WC have such a high permeability that the flow can rapidly go beyond 2 mm and, therefore, the guard ring confines the flow nearly at the start of measurements.

In this investigation, the analytical basis to assess water permeability is the flow-net theory. Different flow patterns will produce different calibration factors, because a calibration factor is solely dependent on the flow-net. The values of the calibration factors for the tests with and without the guard ring were calculated in section 4.1. The steady flow rate can be estimated by regression analysis as shown in section 4.2. As a result, the water permeability coefficients can be determined for both these test conditions.

Table 7 gives the water permeability coefficients according to the flow-net theory. The values of $K_{w\text{-}GR}$ and $K_{w\text{-}No\ GR}$ can be categorised into two groups. In one group, the two permeability values are very close to each other. These results are from the experiments during which the guard ring did not show a significant effect on the flow. For the rest, the values of $K_{w\text{-}GR}$ are always slightly higher than that of $K_{w\text{-}No\ GR}$. This phenomenon is due to the relative difference amongst the calibration factors and the flow rates. Based on section 4.1, the flow rate of a test without the guard ring should be 3.75 times greater than that with the guard ring. The actual experiments, however, show the ratio of two flow rates ranges from 1.69 to 2.24. Therefore, higher permeability coefficients were found in the calculated values for the tests with the guard ring. These effects can be clearly seen in Fig. 15, where the permeability coefficients with and without the guard ring were plotted for each concrete under different curing conditions.

In summary, the influence of the guard ring on flow depended on the permeability properties of the concretes. From the experimental study, there was no justification for using the guard ring because it was not possible to establish a uni-directional flow beyond the near surface region. The experimental results further confirmed a strong correlation between permeability coefficients computed from the flow obtained with and without the guard ring. From a practical point of view, it was found that the success of completing measurements with the guard ring was low. More than 30% of the tests with the guard ring failed and similar observations were also reported by Price and Bamforth (1993). The main problem was in achieving an effective seal between the inner chamber and the outer chamber. The situation was worse in the experimental work reported in this paper because the permeability tests were carried out at 7 bar (0.7 MPa) in contrast to the absorption test, which uses a test pressure of around 0.02 bar (0.002 MPa).

4. Conclusions

The detailed information about the design and development of an instrument for the in-situ water permeability testing is presented and the following conclusions have been drawn on the basis of the analytical and experimental work reported in this paper:

1) The flow simulation has indicated that the guard ring is able to confine the flow at the near surface, but a uni-directional flow is not achievable for the whole depth of the test specimen. The use of a guard ring in a field sorptivity test can be effective, as the water front is limited to the near surface, whilst the ‘same’ hypothesis is questionable for a permeability test that uses a relatively high test pressure.
2) The primary factors influencing the depth of uni-directional water penetration are the size of the inner seal and the size of the guard ring. More importantly, the interaction between the size of the inner seal and that of the guard ring was found to be significant, implying their interdependence needs to be considered whilst assessing the uni-directional flow.
3) A constant flow rate is difficult to obtain, even when the specimens are saturated before testing. However, the variation of flow rates after 60 minutes is relatively small, which was confirmed by the results of the ANOVA. As a result, a steady flow

rate can be considered to have been achieved after 60 minutes in the surface applied water permeability tests that are carried out at a pressure of 7 bar (0.7 MPa).

4) The experimental results show that the effect of the guard ring relies on the concrete mixes and the curing regime. The flow was confined by the guard ring for concretes with porous surface, whilst little or no influence was found for dense concretes.
5) A strong correlation was found between $K_{w\text{-}GR}$ and $K_{w\text{-}NO\ GR}$, although $K_{w\text{-}GR}$ was slightly higher than what the theory predicted. This highlights the validation of the working theory of the new instrument and the viability of carrying out water permeability tests without using the guard ring.
6) An effective seal between the inner and outer chambers with the guard ring arrangement is not easy to achieve due to the high pressure applied and more than 30% of the tests with the guard ring failed. For all the above reasons, the guard ring is not recommended for the surface applied water permeability test.

The laboratory test results reported in this paper indicate the value of the new water permeability test for its potential in situ application. In this paper the basic performance characteristics of the new method have been carefully discussed. Further considerations required for field applications when gradients of both porosity and water content exist in concrete will be studied and reported in future papers.

Acknowledgement

The authors gratefully acknowledge the financial support provided by both the UK Engineering and Physical Sciences Research Council and Queen's University Belfast for carrying out the investigation reported in this paper. The work was carried out entirely at Queen's University Belfast and hence facilities provided by the School of Planning, Architecture and Civil Engineering at Queen's are gratefully acknowledged.

References

Adams, A.E. (1986) Development and application of the CLAM for measureing concrete permeability. PhD thesis, Queen's University Belfast, Belfast, pp. 1-328.

Aïtcin, P.C. (1998) High Performance Concrete. Taylor & Francis.

Arbaoui, T. (1988) Finite Element Calibration of the CLAM. MSc thesis, Queen's University Belfast, Belfast, pp. 1-103.

Bamforth, P.B. (1987) The relationship between permeability coefficients for concrete obtained using liquid and gas. Magazine of concrete research (138):3 –11

Basheer, P.A.M. (1991) 'CLAM' permeability tests for assessing the durability of concrete. PhD thesis, Queen's University Belfast, Belfast, pp. 1-438.

Basheer, P.A.M. (2001) Permeation analysis. In: Ramachandran VS, Beaudoin JJ (eds) Handbook of Analytical Techniques in Concrete Science and Technology: Principles, Techniques and Applications. pp 658-727

Basheer, P.A.M. and Nolan, E.A. (2001) Near-surface moisture gradients and in situ permeation tests. Construction and Building Materials 15:105-114

BS1881-125 (1986) Methods for mixing and sampling fresh concrete in the laboratory. BSI, pp. 1-10.

BS-EN12390 (2000) Testing hardened concrete. Part 8: Depth of penetration of water under pressure. BSI, pp. 1-10.

Cristensen, B.J., Mason, T.O. and Jennings, J.M. (1996) Comparison of measured and calculated permeabilities for hardened cement pastes. Cement and Concrete Research 26:1325-1334

Dhir, R.K., Hewlett, P.C. and Chan, Y.N. (1989) Near surface characteristics of concrete intrinsic permeability. Magazine of Concrete Research 41:87-97

El-Dieb, A.E. and Hooton, R.D. (1995) water permeability measurement of high performance concrete using a high pressure triaxial cell. Cement and Concrete Research 25:1199-1208

Hall, C. (1989) Water sorptivity of mortars and concretes a review. Magazine of Concrete Research 41:51-61

Hearn, N. (1998) Self-sealing, autogenous healing and continued hydration What is the difference. Materials and Structures 31:563-567

Hyde, G.W. and Smith, W.J. (1889) Results of experiments made to determine the permeability of cements and cement mortars. Journal of the Franklin Institute 128:199-207

Long, A.E. (1985) Durability testing of porous material. UK Patent.

Long, A.E., Henderson, G.D. and Montgomery, F.R. (2001) Why assess the properties of near-surface concrete. Construction and Building Materials 15:65-79

Mehta, P.K. and Monteiro, P.J.M. (2006) Concrete: Microstructure, Properties, and Materials. 3rd edn. McGraw Hill.

Montgomery, D.C. (1996) Design and Analysis of Experiments. 4 edn. John Wiley & Sons,

Neville, A.M. (1996) Properties of concrete. 4th edn. John Wiley&Sons,

Nolan, E., Ali, M.A., Basheer, P.A.M. and Marsh, B.K. (1997, January/February), Testing the effectiveness of commonly used site curing regimes, Materials and Structures, 30, pp 53-60.

Parrott, L.J. and Hong, C.Z. (1991) Some factors influecing air permeation measurements in cover conrete. Materials and Structures 24:403-408

Perry, M. and Hollis, D. (2003) The generation of monthly gridded datasets for a range of climatic variables over the United Kingdom. Met Office.

Price, W.F. and Bamforth, P.B. (1993) Initial surface absorption of concrete: Examination of modified test apparatus for obtaining uniaxial absorption. Magazine of Concrete Research 45:17-24

Stanish, K.D., Hooton, R.D. and Thomas, M.D.A. (2000) Testing the Chloride Penetration Resistance of Concrete: A Literature Review. FHWA Contract DTFH61-97-R-00022 "Prediction of Chloride Penetration in Concrete".

Torrent, R.T. (1992) A two-chamber vacuum cell for measuring the coefficient of permeability to air of the concrete cover on site. Materials and Structures 25:358-365

TR-31 (2008) Permeability testing of site concrete. Concrete Society, pp. 1-90.

Yang, K., Basheer, P.A.M., Long, A.E. and Bai, Y. (2012) Assessment of air permeability of high performance concretes using a new in situ test. 3rd International conference on the durability of concrete structures, 17-19 September, Queen's University Belfast, Belfast, pp 1-8.

Table 1 Basic input parameters of the models

Parameters	Level	Note
Permeability	10^{-14} ms^{-1}	Typical K_w for HPCs
Specimen dimension	500×500×200 mm	To simulate the real condition
Testing pressure	7 bar (0.7 MPa)	The same value as DIN-1048
Testing area	Diameter: 50 mm	The same as CLAM water test
Saturation degree	Fully saturated	Assumption
Test state	Steady state	Assumption

Table 2 2^3 central point factorial experiment (coded unit)

Level / Factor	-1	+1
A: Inner seal (IS) size	5mm	15mm
B: Guard ring (GR) size	10mm	50mm
C: Outer seal (OS) size	10mm	30mm

Note: the central point has IS: 10mm, GR: 30mm and OS: 20mm.

Table 3 Estimated effects and coefficients for uni-direction depth (coded units)

Term	Effect	Coef	SE Coef	t-statistic	P-value
Constant		1.028	0.0064	160.4	<0.001**
Inner seal (IS)	-0.366	-0.183	0.0064	-28.5	<0.001**
Guard ring (GR)	0.239	0.120	0.0064	18.64	<0.001**
Outer seal (OS)	0.031	0.015	0.0064	2.40	0.043*
IS×GR	-0.123	-0.065	0.0064	-10.08	<0.001**
IS×OS	-0.019	-0.009	0.0064	-1.48	0.177
GR×OS	-0.007	-0.004	0.0064	-0.59	0.570
IS×GR×OS	0.0014	0.0007	0.0064	0.11	0.917

Note: * effects significant, p-value: 1%-5%.
** effects highly significant, p-value:<1%.

Table 4 Experimental Variables

Variables	Levels
Concrete mix	C20, C40, C60, C80
Curing regimes	AC: Air curing for 90 days WC: Water curing for 3 days and then air cured for 90 days SC: Continuously water cured for 90 days
Test condition	With application of the guard ring Without the application of the guard ring

Table 5 Mix proportions and general properties of concrete tested in this study

Concrete	C20	C40	C60	C80
Water (kg/m^3)	256	192	145	145
Portland cement* (kg/m^3)	375	375	388	449
Microsilica* (kg/m^3)	0	0	0	36
PFA* (kg/m^3)	0	0	97	97
Sand*** (kg/m^3)	625	685	668	652
Coarse aggregate*** (kg/m^3)	1136	1245	1150	1150
Superplasticiser** (%)	0	0.8	1.4	1.5
Air content (%)	1.2	1.3	0.6	1.6
Slump (mm)	180	185	220	240
28 day compressive strength (MPa)	24.1	52.1	81.3	84.2
56 day compressive strength (MPa)	33.7	59.8	90.7	94.6

Note: * CEM I manufactured by Quinn cement, Northern Ireland, PFA from Kilroot Power station in Northern Ireland, and Microsilica in the form of slurry from Elkem were used.

** Superplasticiser was CHEMCRETE HP 3 manufactured by Larsen Limited, Northern Ireland and it refers to percentage of binder content.

*** The fine aggregate was medium graded natural sand and the coarse aggregate was crushed basalt.

Table 6 Analysis of variance (ANOVA) of flow rates after 60 minutes

Source	Degree of freedom	Sum of squares	Mean square	$F_{3,8}$	P-value
Factor	3	0.0207	0.0069	0.65	0.604
Error	8	0.0847	0.0106		
Total	11	0.1055			

Table 7 Summary of the results of permeability coefficients (10^{-14} m/s)

Concrete mix	Curing regime	$K_{w\text{-}GR}$	$K_{w\text{-}No\ GR}$
C20	SC	0.272	0.253
	WC	36.833	16.500
	AC	373.333	205.000
C40	SC	0.142	0.131
	WC	2.433	1.330
	AC	8.150	3.733
C60	SC	0.070	0.084
	WC	0.195	0.205
	AC	0.612	0.363
C80	SC	0.062	0.062
	WC	0.144	0.163
	AC	0.212	0.243

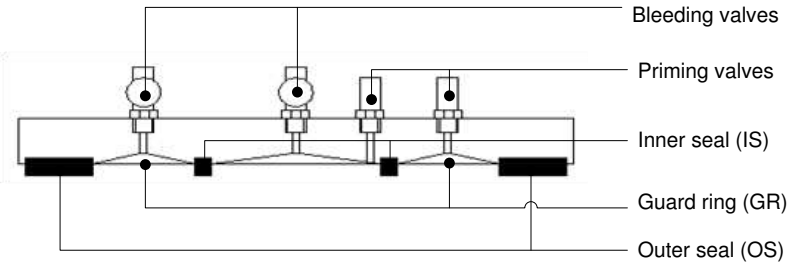

Fig. 1 The details of test head with guard ring

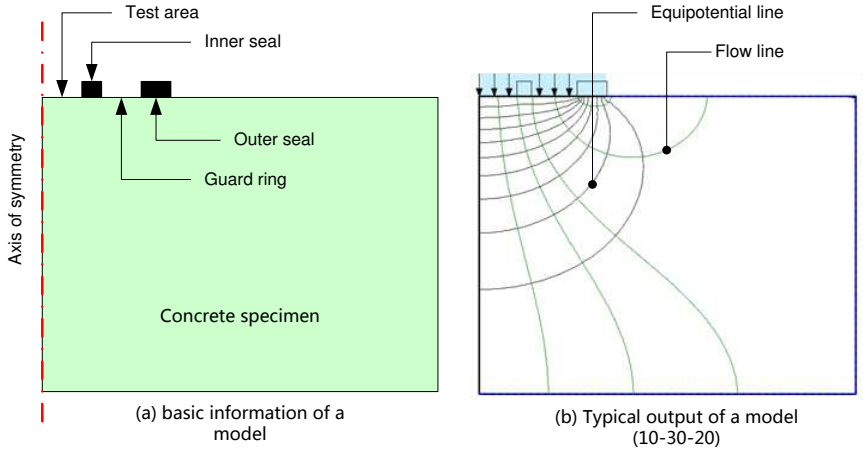

Fig. 2 Illustration of basic information and a flow-net determined from a model

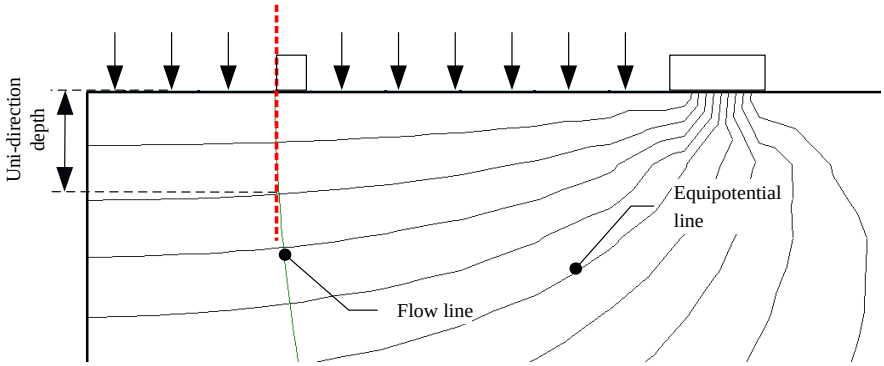

Fig. 3 Method to determine uni-directional depth based on the output of the model

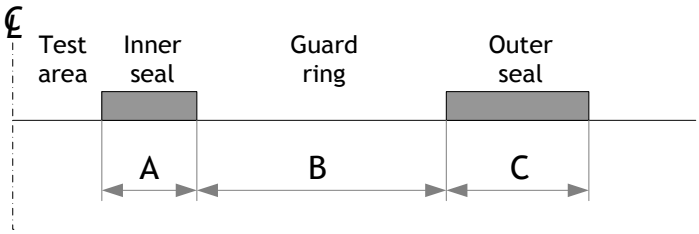

Fig. 4 The definition of the relevant dimensions of the inner seal, the guard ring and the outer seal in the model

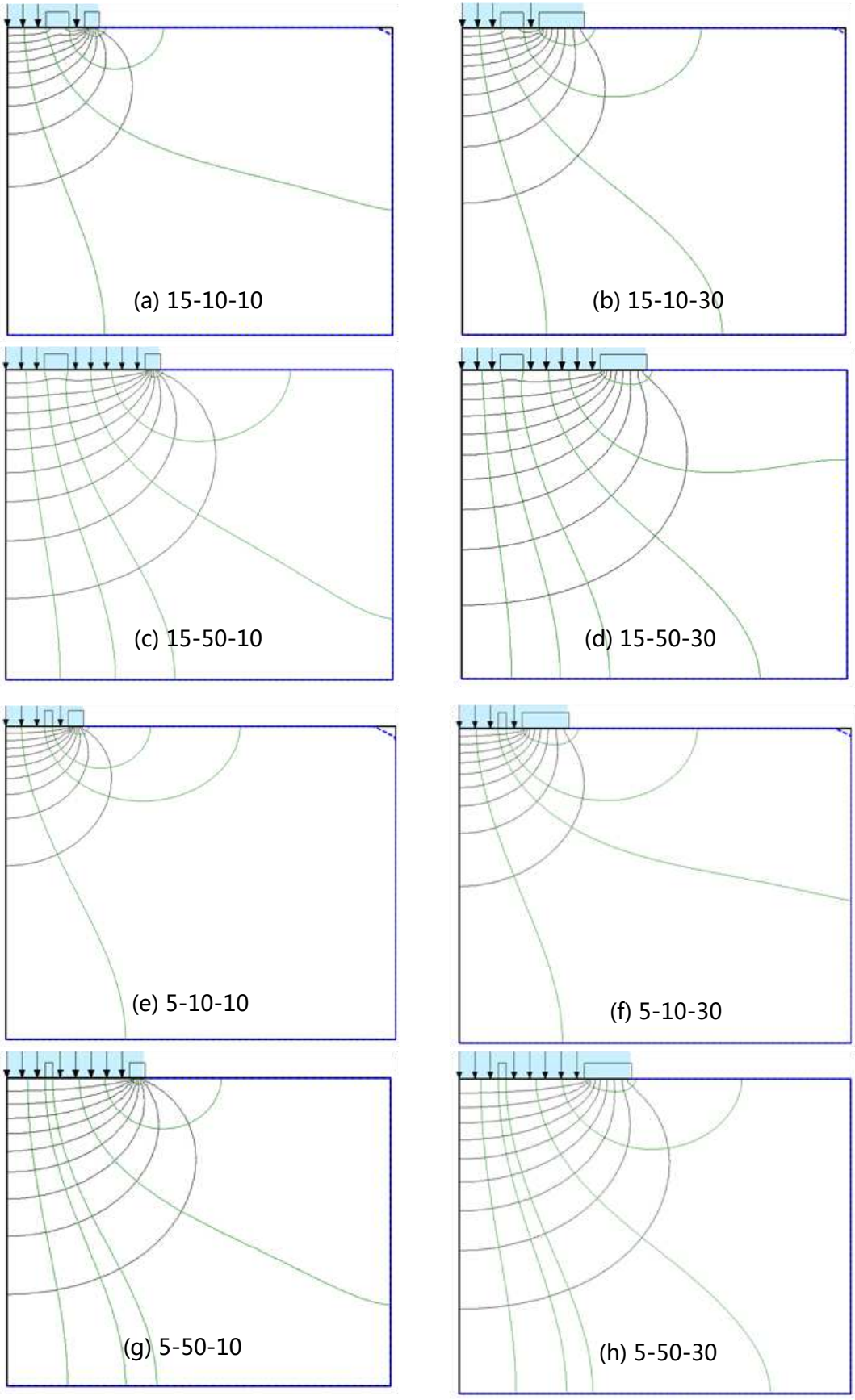

Fig. 5 Flow-nets of the eight setups determined from the computer simulation

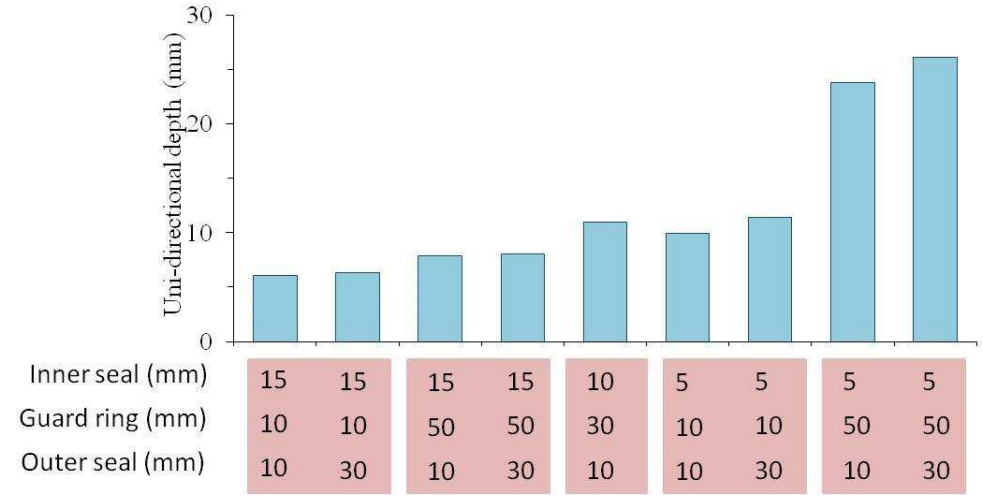

Fig. 6 Depth of uni-directional flow for different set-ups

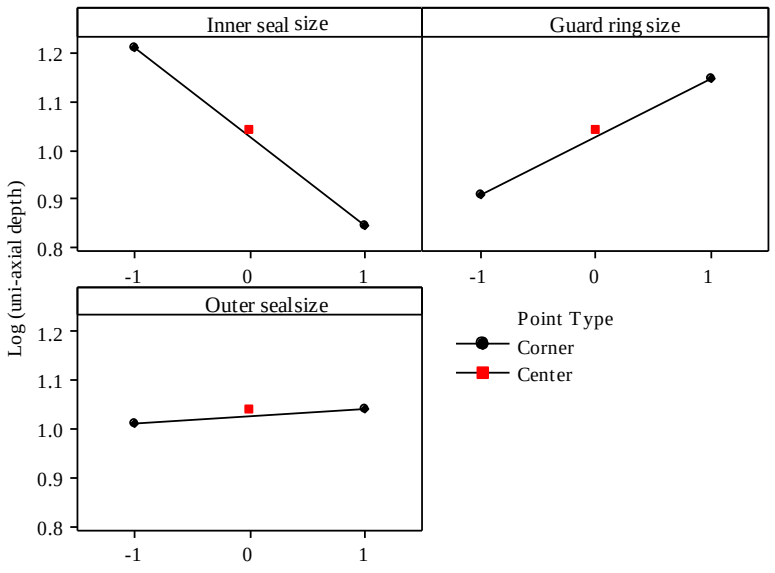

Fig. 7 The plots of main effects of three factors (IS, GR, OS)

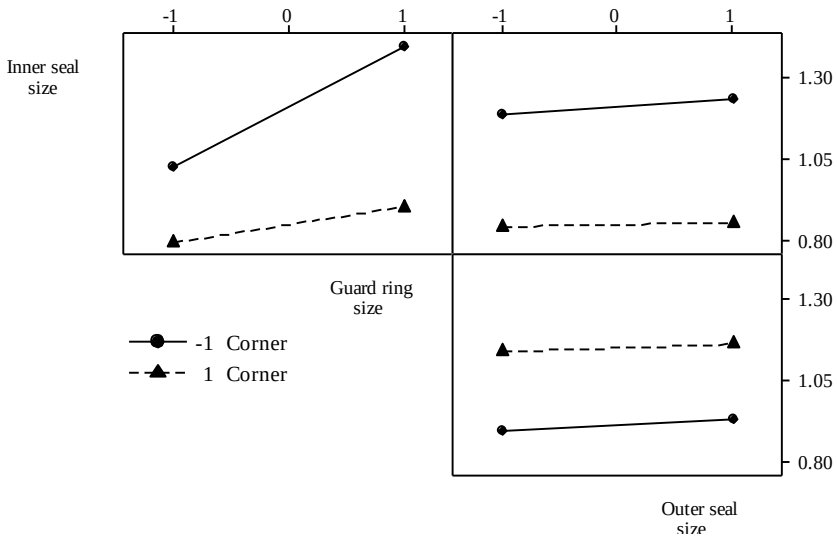

Fig. 8 The plots of the interactions between the three factors

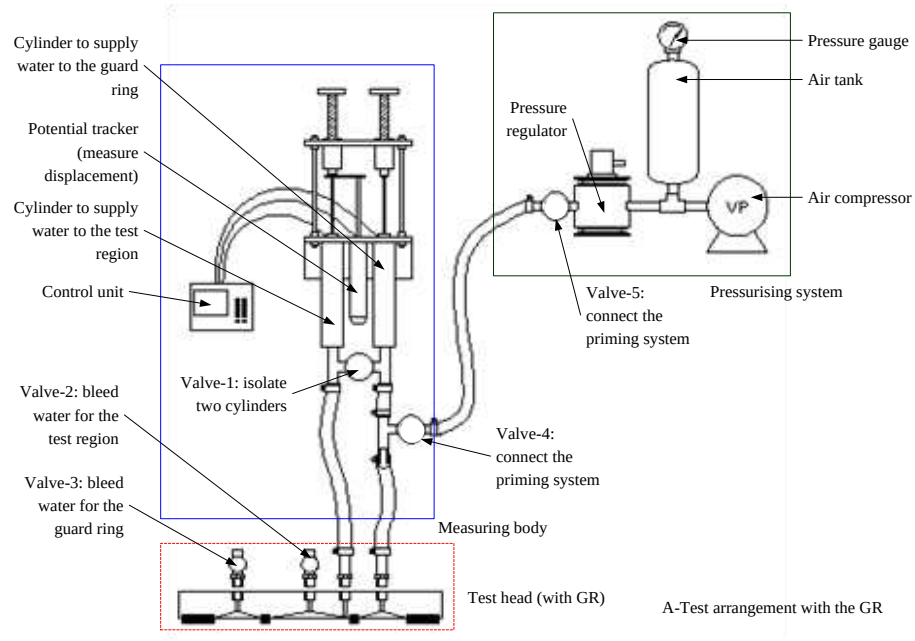

(a) WITH the guard ring

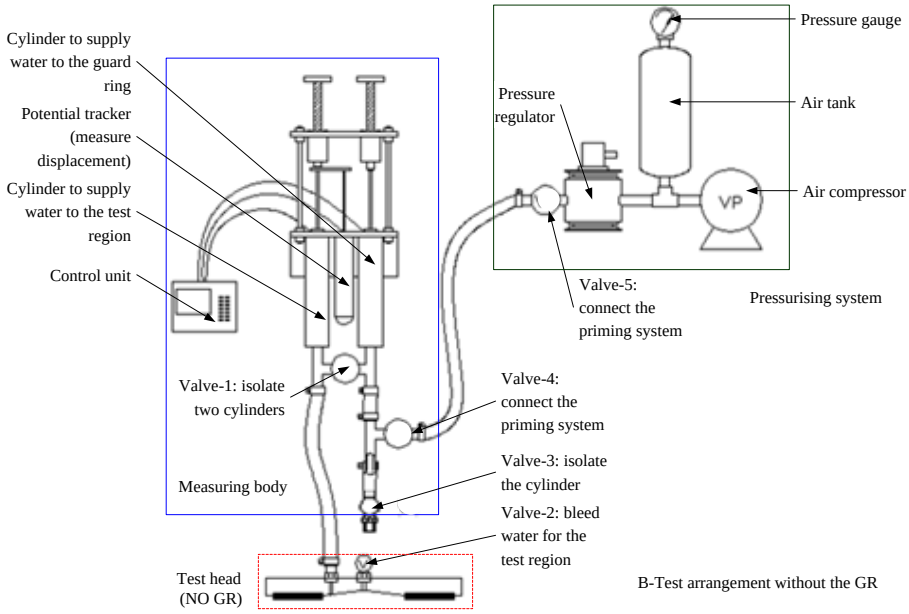

(b) WITHOUT the guard ring

Fig. 9 Schematic of the high pressure surface mounted water permeability test

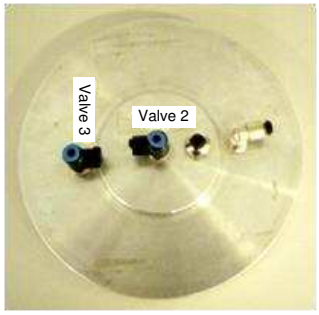

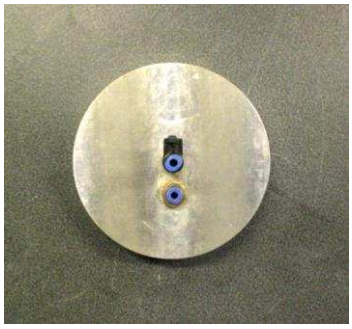

(a) The test head with the guard ring (b) The test head without the guard ring

(c) Clamped test heads to confirm water tightness

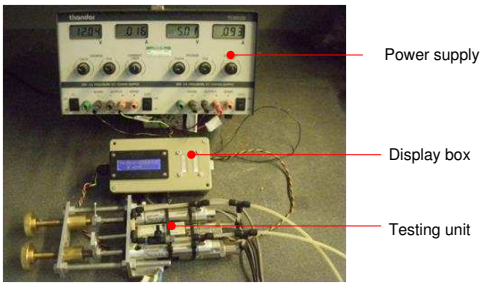

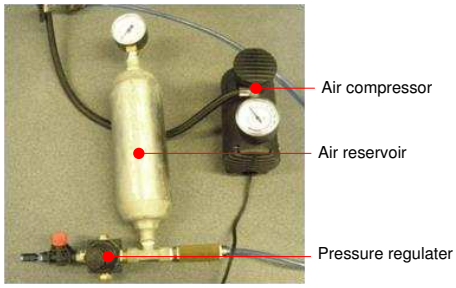

(d) The measuring unit of the instrument (e) The priming system

Fig. 10 The test heads, the measuring unit and the priming system of the instrument

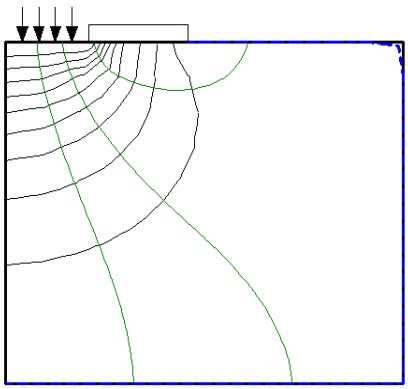

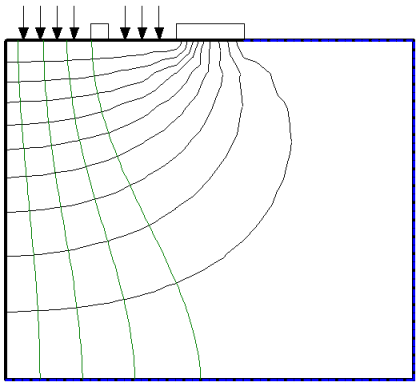

(a) Flow-net without GR (b) Flow-net with GR

Fig. 11 Presentation of the flow-nets with and without guard ring

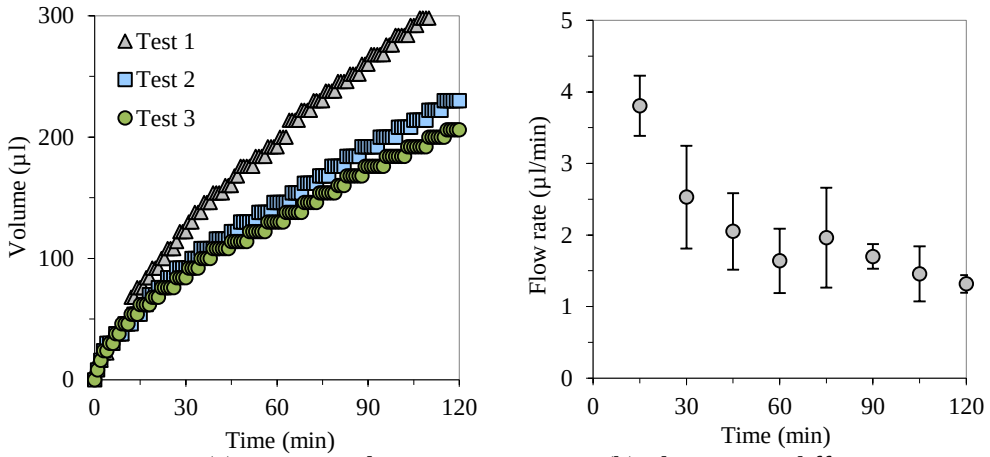

(a) Test record (b) Flow rate at different time

Fig. 12 Graphical interpretation of flow rates

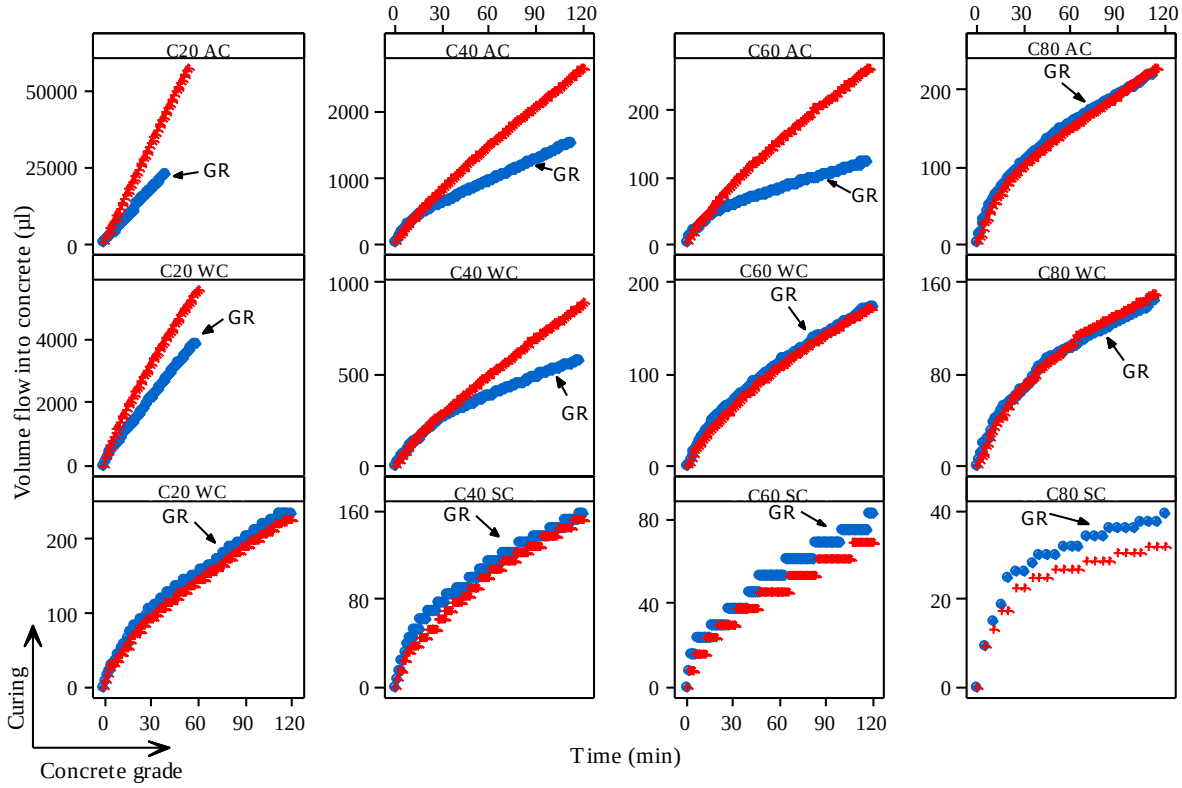

Fig. 13 Original data for 4 concretes after 3 different curing regimes with and without the guard ring

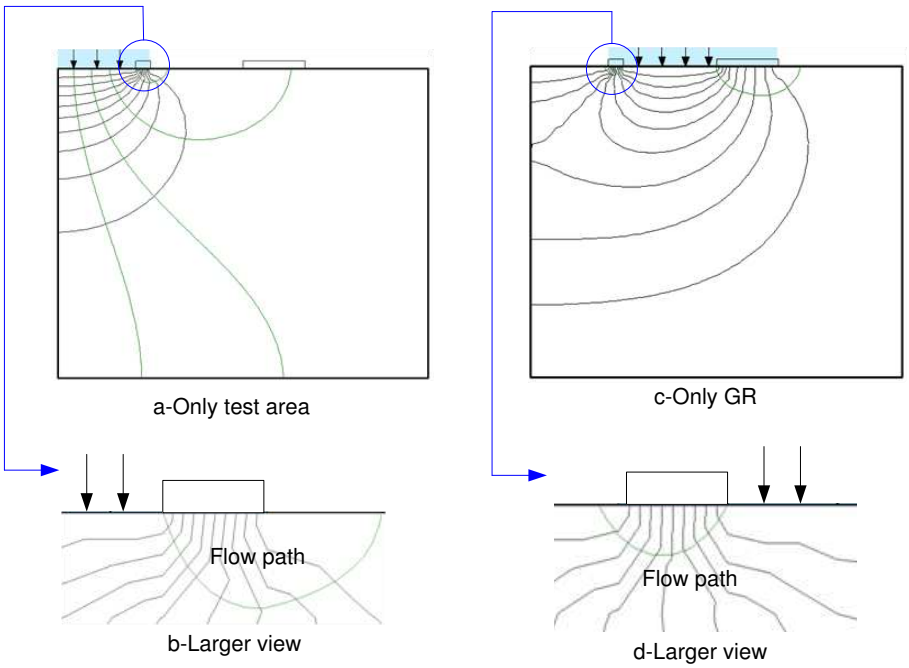

Fig. 14 The flow-net of two models where a pressure was applied in the test area and the guard ring separately

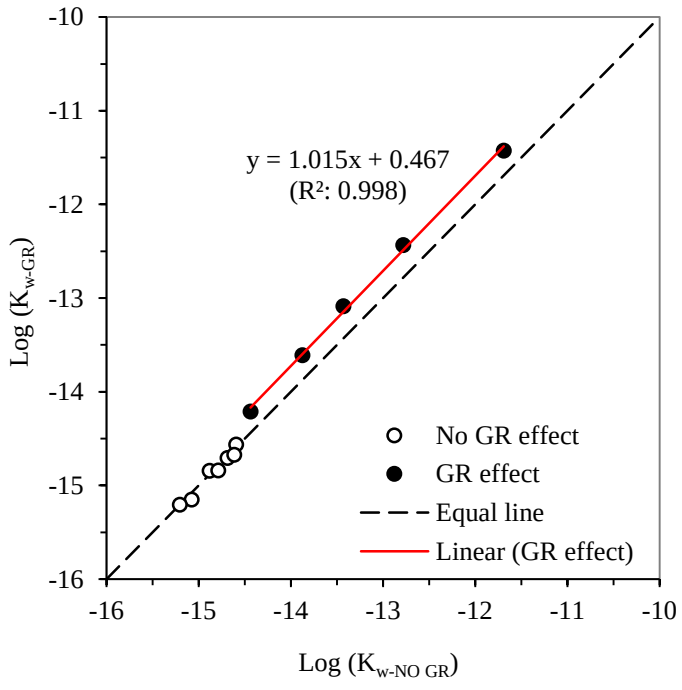

Fig. 15 The relationship between $K_{w\ GR}$ and $K_{w\ No\ GR}$